

# Cyclophilin D Deficiency Rescues Axonal Mitochondrial Transport in Alzheimer's Neurons

Lan Guo<sup>1</sup>, Heng Du<sup>1</sup>, Shiqiang Yan<sup>1,2</sup>, Xiaoping Wu<sup>3</sup>, Guy M. McKhann<sup>3</sup>, John Xi Chen<sup>4</sup>, Shirley ShiDu Yan<sup>1\*</sup>

**1** Department of Pharmacology & Toxicology and Higuchi Bioscience Center, School of Pharmacy, University of Kansas, Lawrence, Kansas, United States of America, **2** College of Chemistry and Chemical Engineering, Lanzhou University, Lanzhou, Gansu, People's Republic of China, **3** Department of Neurosurgery, Physicians & Surgeons College of Columbia University, New York, New York, United States of America, **4** Department of Neurology, Memorial Sloan-Kettering Cancer Center, New York, New York, United States of America

## Abstract

Normal axonal mitochondrial transport and function is essential for the maintenance of synaptic function. Abnormal mitochondrial motility and mitochondrial dysfunction within axons are critical for amyloid  $\beta$  ( $A\beta$ )-induced synaptic stress and the loss of synapses relevant to the pathogenesis of Alzheimer's disease (AD). However, the mechanisms controlling axonal mitochondrial function and transport alterations in AD remain elusive. Here, we report an unexplored role of cyclophilin D (CypD)-dependent mitochondrial permeability transition pore (mPTP) in  $A\beta$ -impaired axonal mitochondrial trafficking. Depletion of CypD significantly protects axonal mitochondrial motility and dynamics from  $A\beta$  toxicity as shown by increased axonal mitochondrial density and distribution and improved bidirectional transport of axonal mitochondria. Notably, blockade of mPTP by genetic deletion of CypD suppresses  $A\beta$ -mediated activation of the p38 mitogen-activated protein kinase signaling pathway, reverses axonal mitochondrial abnormalities, improves synaptic function, and attenuates loss of synapse, suggesting a role of CypD-dependent signaling in  $A\beta$ -induced alterations in axonal mitochondrial trafficking. The potential mechanisms of the protective effects of lacking CypD on  $A\beta$ -induced abnormal mitochondrial transport in axon are increased axonal calcium buffer capability, diminished reactive oxygen species (ROS), and suppressing downstream signal transduction P38 activation. These findings provide new insights into CypD-dependent mitochondrial mPTP and signaling on mitochondrial trafficking in axons and synaptic degeneration in an environment enriched for  $A\beta$ .

**Citation:** Guo L, Du H, Yan S, Wu X, McKhann GM, et al. (2013) Cyclophilin D Deficiency Rescues Axonal Mitochondrial Transport in Alzheimer's Neurons. PLoS ONE 8(1): e54914. doi:10.1371/journal.pone.0054914

**Editor:** Javier Vitorica, Universidad de Sevilla, Spain

**Received:** September 26, 2012; **Accepted:** December 17, 2012; **Published:** January 31, 2013

**Copyright:** © 2013 Guo et al. This is an open-access article distributed under the terms of the Creative Commons Attribution License, which permits unrestricted use, distribution, and reproduction in any medium, provided the original author and source are credited.

**Funding:** This study was supported by grants from National Institute of Aging (R37AG037319 and K99AG037716) and the Alzheimer's Association. The funders had no role in study design, data collection and analysis, decision to publish, or preparation of the manuscript.

**Competing Interests:** The authors have declared that no competing interests exist.

\* E-mail: shidu@ku.edu

These authors contributed equally to this work.

## Introduction

Neurons are highly polarized cells with axons projecting from the cell body to transmit interneuronal information. Axons rely on axonal transport to deliver most essential proteins and membrane bound organelles [1,2]. Among the many types of axonal transport cargo, mitochondria play an essential role in supporting synaptic activity and plasticity due to their ability to generate ATP and meticulously regulate local calcium homeostasis [3–5]. The saltatory and bidirectional transports of mitochondria accumulate axonal mitochondria around structures such as presynapses and growth cones where there are high energy demand and constant calcium fluctuation [6–8], suggesting the close relationship of mitochondrial function, transport and positioning [9].

Indeed, concomitant mitochondrial dysfunction and motility change has been observed in neurodegenerative diseases including Alzheimer's disease (AD) [10]. As a major causative factor of AD, amyloid beta ( $A\beta$ ) particularly its oligomeric form, exerts multiple effects on mitochondrial function including intra-mitochondrial  $A\beta$  accumulation, decreased mitochondrial respiration and membrane potential, impaired permeability transition, and in-

creased production of mitochondrial reactive free radicals [11–19]. Our recent studies indicate that mitochondria at synapses including axonal mitochondria are early victims of  $A\beta$  toxicity along with alterations in axonal mitochondrial movement [20–22]. More recently, emerging studies accentuated alterations in axonal mitochondrial motility and dynamics in  $A\beta$ -rich environments and suggest axonal mitochondrial motility change is closely correlated to synaptic dysfunction in AD neurons [22–26]. It thus raises an intriguing question of whether  $A\beta$ -induced mitochondrial dysfunction contributes to changes in axonal mitochondrial motility. The specific mechanisms underlying  $A\beta$ -induced impairment in axonal mitochondrial transport have not been fully elucidated.

Cyclophilin D (CypD; gene: Ppif) is a key component of mitochondrial permeability transition pore (mPTP) that consists of the voltage dependent anion channel (VDAC) in the outer mitochondrial membrane, the adenine nucleotide translocase (ANT) in the inner membrane, and cyclophilin D (CypD) in the mitochondrial matrix. Release of CypD from matrix allows it to bind to the ANT and VDAC to trigger the opening of mPTP. The opening of mPTP constitutes non-selective, high conductance pore allowing transport of not only calcium by any solute below the

pore size. This results in mitochondrial osmotic swelling and dissipation of mitochondrial membrane potential, reduced mitochondrial calcium retention capacity; decreased membrane potential; increased reactive oxygen species (ROS) production; and eventually, cell death [13,27,28]. Accordingly, we have demonstrated that the blockade of CypD significantly attenuates mPTP-related mitochondrial dysfunction and cognitive impairments in an AD mouse model [12,29], suggesting the protective effect of CypD depletion against A $\beta$ -associated synaptic degeneration. However, it remains unclear whether CypD-dependent mPTP leading to mitochondrial dysfunction is linked to A $\beta$ -induced damage of axonal mitochondrial transport. If so, does blockade of mPTP via CypD depletion attenuate impaired mitochondrial transport and protect from A $\beta$  toxicity? Given the close relationship of mitochondrial function with transport and the critical role of normal mitochondrial distribution in sustaining synaptic plasticity and strength, it is essential and logical to delineate the role of CypD in mitochondrial trafficking in axons in A $\beta$  rich environment. The outcome of this study on axonal mitochondrial transport deepened our understanding of the impact of Cyclophilin D related perturbations on mitochondrial function and added to the body of CypD-dependent mechanisms underlying A $\beta$ -induced mitochondrial and synaptic degeneration [12,29].

The goal of the present study is to determine the effect of CypD on A $\beta$ -induced axonal mitochondrial trafficking and synaptic damage. We demonstrate that the blockade of mPTP by CypD depletion rescues axonal mitochondrial trafficking and protects synapse from A $\beta$  toxicity. The potential mechanisms underlying the protection of CypD deficiency on axonal mitochondrial trafficking are related to the suppression of A $\beta$ -induced calcium perturbation and accumulation of axonal reactive oxygen species (ROS), and activation of downstream signal P38/MAPK pathway. These studies delineate new insights into the crosstalk of CypD-dependent mPTP and axonal mitochondrial transport, contributing to the synaptic pathophysiology in AD pathogenesis, especially related to A $\beta$ -induced axonal mitochondrial injury.

## Methods

### Ethics Statement

This study was performed in strict accordance with the recommendations in the Guide for the Care and Use of Laboratory Animals of the National Institutes of Health. The protocol was approved by the Committee on the Ethics of Animal Experiments of the University of Kansas (IACUC protocol number: 203-01).

### Mice

Animal studies were approved by the Animal Care and Use Committee of University of Kansas in accordance with the National Institutes of Health guidelines for animal care. CypD homozygous null mice (*Ppif*<sup>-/-</sup>) were kind gifts from Dr. Jeffery D. Molkentin. These animals were backcrossed 10 times into the C57BL6 background.

### Neuronal Culture

Mouse hippocampal neurons were cultured as previously described [20].

### Preparation of Oligomeric A $\beta$

Oligomeric A $\beta$ 1-42 was prepared as previously described [20].

## Axonal Mitochondrial Trafficking Recording and Data Analysis

These recordings were performed using previously reported protocols [20]. Axonal processes were determined by morphological characteristics and confirmed by Tau-1 retrospect staining as previously described [20]. To be more specific, a process that is two to three times longer than other processes stemming from the soma is considered to be an axon; besides, neurons were subjected to retrospect staining of Tau-1, which is abundant in axons and is widely accepted as axonal marker [20,30–32]. The images were taken before and after treatment with 200 nM oligomer A $\beta$  (24 hr), and/or 1  $\mu$ M SB203580 (24 hr), 5  $\mu$ M Probuco (24 hr) or 5  $\mu$ M A23187 (30 minutes).

### Treatment of Cyclosporine A

Cyclosporin A (CsA, Sigma) at a final concentration of 500 nM was added to the cells 30 min prior to oligomeric A $\beta$  treatment.

### Measurement of Mitochondrial Intra-axonal Ca<sup>2+</sup> and ROS

Neurons were loaded with 1  $\mu$ M Fluo-4 AM (Invitrogen) for 30 minutes to monitor changes in intracellular Ca<sup>2+</sup> or 10  $\mu$ M dichlorodihydrofluorescein (H2-DCF) to detect ROS. Fluorescence images were captured using the inverted Zeiss Axiovert 200 microscope with a stage based chamber (5% CO<sub>2</sub>, 37°C). Images were analyzed using Image J software. Background fluorescence was calculated by sampling the areas that were around the measured axons, but had no axons in these fields and background intensity was subtracted from the raw data.

### Immunoblotting Analysis

Samples were lysed in extraction buffer (10 mM Tris-HCl pH 7.4, 100 mM sodium chloride, 1 mM EDTA, 1 mM EGTA, 1 mM sodium fluoride, 20 mM sodium pyrophosphate, 2 mM sodium orthovanadate, 1% Triton X-100, 10% glycerol, 0.1% SDS, 0.5% deoxycholate, 1 mM PMSF) containing protease inhibitor cocktail (Calbiochem, set V, EDTA free), separated by SDS-PAGE (12% Bis-tris gel, Invitrogen), and then transferred to nitrocellulose membrane (Amersham). After blocking in TBST buffer (20 mM Tris-HCl, 150 mM sodium chloride, 0.1% Tween-20) containing 5% nonfat dry milk (Santa Cruz) for 1 hr at room temperature, the membrane was incubated and gently shaken overnight (at 4°C) with primary antibodies. This was followed by incubation with corresponding secondary antibody for 1 hr at room temperature. Chemiluminescence was detected using an electrochemiluminescence instrument (GE). The following antibodies were used in this experiment: mouse anti-phospho (pT180/pY182) -p38 (BD Biosciences), rabbit anti-p38 (Cell signaling technology), goat anti mouse IgG HRP conjugated and goat anti rabbit IgG HRP conjugated (Invitrogen). NIH image J software was utilized to analyze the scanned blots and to quantify the intensity of immunoreactive bands.

### Electrophysiological Recording

Recordings were performed at 30°C as described in the previous reports [33,34]. Cells were continuously perfused with oxygen saturated artificial cerebrospinal fluid (ACSF) containing 1  $\mu$ M TTX and 50  $\mu$ M picrotoxin at a rate of 2 ml/min. Patch pipettes were filled with intrapipette solution containing 130 mM K-gluconate, 5 mM KCl, 10 mM HEPES, 2.5 mM MgCl<sub>2</sub>, 10 mM K-phosphocreatine, 4 mM MgATP and 0.6 mM EGTA, pH 7.3. Recording pipettes were prepared on a pipette puller

(Sutter) and had a resistance of 2.5–4 M $\Omega$  when filled with intrapipette solution. Seal was performed on clearly visualized neuron bodies with 10–20  $\mu\text{m}$  diameters. The spontaneous miniature excitatory postsynaptic currents (mEPSCs) were recorded at holding potential at  $-70$  mV using MultiClamp 700A (Axon Instruments) and events were analyzed using Axon clampfit (Axon Instrument, version 8.2.0.235) and MiniAnalysis 6.0 (Synaptosoft).

### Neuronal Synaptic Density

Synaptic density of cultured neurons was measured by counting synaptophysin clusters attaching to neuronal dendrites and presented as the numbers of synaptophysin clusters per micron of dendrite. Neurons were fixed in 4% paraformaldehyde for 20 minutes and then blocked in 10% goat serum for 30 minutes. Synaptophysin was visualized by rabbit anti-synaptophysin IgG (Dako) followed by goat anti-rabbit IgG conjugated with TRITC (Sigma – Aldrich Corp.). Neuronal dendrites were visualized by mouse anti-MAP2 IgG (Boehringer Mannheim) followed by goat anti-mouse IgG conjugated with FITC (Sigma – Aldrich Corp.). Images were taken under a Biorad confocal and analyzed by NIH Image J program.

### Statistical Analysis

One-way ANOVA was used for repeated measure analysis.  $P < 0.05$  was considered significant. Post-hoc ANOVA was used when appropriate. STATVIEW statistics computer software was utilized. All data were expressed as mean  $\pm$  Standard Error of the Mean (SEM).

## Results

### Loss of CypD Attenuates A $\beta$ -induced Changes in Axonal Mitochondrial Motility and Dynamics

Axonal mitochondria are distributed along axons (Fig. S1) and decreased axonal mitochondrial density is a manifestation of disrupted mitochondrial trafficking. To determine the direct effect of CypD, we compared axonal mitochondrial distribution between cultured nonTg and CypD-deficient (*Ppif*<sup>-/-</sup>) hippocampal neurons after exposure to 200 nM oligomeric A $\beta$ 1-42 or rA $\beta$  (reversed sequence of A $\beta$ 1-42) for 24 hours to mimic low *in vivo* levels and chronic A $\beta$  insults in AD brain. Following A $\beta$  treatment, nonTg neurons revealed significantly decreased axonal mitochondrial density (vehicle:  $0.236 \pm 0.01/\mu\text{m}$  vs. A $\beta$ :  $0.188 \pm 0.01/\mu\text{m}$ ) (Fig. 1A). In contrast, CypD depletion protected axonal mitochondrial density from A $\beta$  toxicity (Fig. 1A; A $\beta$ :  $0.246 \pm 0.01/\mu\text{m}$  vs. vehicle:  $0.254 \pm 0.019/\mu\text{m}$ ). Axonal mitochondrial density showed no significant changes in vehicle-treated nonTg neurons when compared to *Ppif*<sup>-/-</sup> neurons (Fig. 1A), suggesting no effect of CypD depletion on axonal mitochondrial distribution without A $\beta$  insults. The addition of control reversed A $\beta$ 42-1 (rA $\beta$ ) did not affect axonal mitochondrial density in nonTg or *Ppif*<sup>-/-</sup> neurons (Fig. 1A). These results indicate that CypD depletion preserves the organization of axonal mitochondrial distribution following A $\beta$  insults.

We next investigated patterns of axonal mitochondrial movement. Mitochondria in the middle region of the axon were utilized for the study of movement patterns (movable or stationary) and movement direction (anterograde or retrograde) as previously described [20]. Mitochondria with displacement more than its length ( $\sim 2$   $\mu\text{m}$ ) during a 120 second recording were considered to be movable; less movement was considered as ‘stationary.’ Among the mitochondria that showed movement, those exhibiting displacement towards the distal end of the axon at the end of

the recording period were termed anterograde mitochondria, while those showing movement to the proximal end were termed retrograde mitochondria.

To objectively examine movement changes following A $\beta$  treatment, we first measured baseline (vehicle treatment) movement patterns. The percentage of stationary mitochondria among total mitochondria in nonTg neurons was comparable to those in *Ppif*<sup>-/-</sup> neurons (Fig. 1B; nonTg:  $58.30 \pm 1.32\%$  vs. *Ppif*<sup>-/-</sup>:  $60.22 \pm 0.92\%$ ), suggesting no effect of CypD depletion on normal docking of mitochondria. However, the percentage of stationary mitochondria increased by 1.3 fold in A $\beta$ -treated nonTg neurons (Fig. 1B, 1E; A $\beta$ :  $73.40 \pm 2.34\%$  vs. vehicle:  $58.30 \pm 1.32\%$ ), but not in *Ppif*<sup>-/-</sup> neurons (Fig. 1B, 1E; A $\beta$ :  $62.30 \pm 1.45\%$  vs. vehicle:  $60.22 \pm 0.92\%$ ). These data indicate that the absence of CypD reverses A $\beta$ -induced impairments in mitochondrial trafficking within axonal processes.

We then analyzed the direction of mitochondrial transport. Consistent with previous results [20,24,26], A $\beta$  treatment significantly reduced the percentage of anterograde (Fig. 1C1, 1E; from  $24.8 \pm 1.44\%$  to  $13.1 \pm 1.34\%$ ) and retrograde mitochondria (Fig. 1C2, 1E; from  $17.52 \pm 1.28\%$  to  $12.91 \pm 0.92\%$ ) compared to vehicle-treated nonTg or *Ppif*<sup>-/-</sup> neurons. CypD-deficient neurons showed increases in both anterograde and retrograde mitochondrial movement in the face of A $\beta$  toxicity as compared to A $\beta$ -treated nonTg neurons (Fig. 1C1–2, 1E; anterograde:  $21.55 \pm 1.59\%$ ; retrograde:  $16.15 \pm 0.87\%$ ).

Next, we examined the velocity of mitochondrial movement. Compared to vehicle-treated control, A $\beta$  treatment decreased anterograde velocity of nonTg mitochondria by 26% (Fig. 1D1, 1E; A $\beta$ :  $0.287 \pm 0.018$  vs. vehicle:  $0.388 \pm 0.016$   $\mu\text{m}/\text{sec}$ ), while the anterograde velocity of *Ppif*<sup>-/-</sup> mitochondria was preserved in conditions of A $\beta$  toxicity (Fig. 1D1, 1E;  $0.435 \pm 0.022$   $\mu\text{m}/\text{sec}$ ). Vehicle treatment alone for nonTg and *Ppif*<sup>-/-</sup> mitochondria demonstrated comparable anterograde velocity (Fig. 1D1; nonTg:  $0.388 \pm 0.016$  vs. *Ppif*<sup>-/-</sup>:  $0.422 \pm 0.017$   $\mu\text{m}/\text{sec}$ ). Analysis of cumulative distribution data revealed a leftward shift in the velocity curve for A $\beta$ -treated anterograde nonTg mitochondria (Fig. 1D2), while velocity in A $\beta$ -treated *Ppif*<sup>-/-</sup> anterograde mitochondria was not shifted as compared with vehicle-treated mitochondria (Fig. 1D3). Consistent with our previous results [20], A $\beta$  treatment did not significantly impact the velocity of nonTg retrograde mitochondria when compared to vehicle-treatment (Fig. 1D4; vehicle:  $0.381 \pm 0.016$  vs A $\beta$ :  $0.362 \pm 0.032$   $\mu\text{m}/\text{sec}$ ). Further, the velocity of *Ppif*<sup>-/-</sup> retrograde mitochondria was also not affected by A $\beta$  insults (Fig. 1D4; vehicle:  $0.450 \pm 0.022$  vs A $\beta$ :  $0.419 \pm 0.015$   $\mu\text{m}/\text{sec}$ ). As a control, the addition of rA $\beta$  did not significantly change directional mitochondrial movement in nonTg or *Ppif*<sup>-/-</sup> neurons (Fig. 1B–1D4). Taken together, these data indicate that CypD depletion significantly protects directional mitochondrial transport from the effects of A $\beta$  toxicity.

### Effect of CypD Depletion on A $\beta$ -instigated Axonal Mitochondrial Fragmentation

To evaluate changes in mitochondrial morphology, we measured the average length of axonal mitochondria. A $\beta$  treatment decreased the average length of nonTg axonal mitochondria by 34.3% (Fig. 2A;  $1.421 \pm 0.022$   $\mu\text{m}$  in vehicle groups vs.  $0.933 \pm 0.037$   $\mu\text{m}$  in A $\beta$ -treated groups). Cumulative distribution data showed that A $\beta$  treatment caused a remarkable increase in the number of small mitochondria and a decrease in the number of long mitochondria in nonTg neurons (Fig. 2B). Although *Ppif*<sup>-/-</sup> mitochondria demonstrated a 14.9% decrease in average length following A $\beta$  exposure as compared to the corresponding in

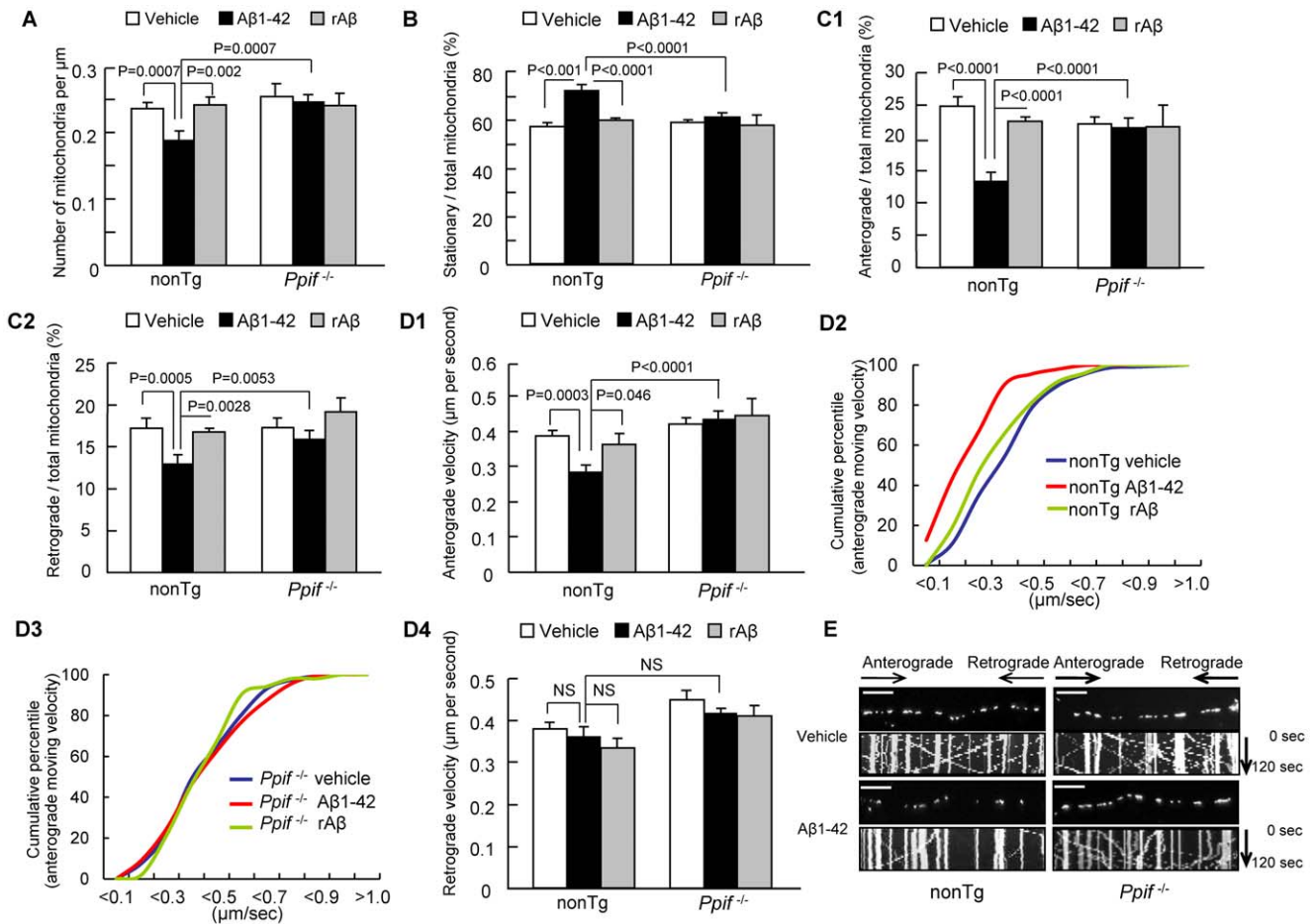


**Figure 1. Loss of CypD protects axonal mitochondrial motility and dynamics from Aβ toxicity.** (A) CypD depletion increased axonal mitochondrial density (numbers per micron of axon) in Aβ-treated neurons. rAβ: reversed Aβ42-1. There is no significant difference in the axonal mitochondrial density between vehicle-treated nonTg and *Ppif*<sup>-/-</sup> neurons. Data were collected from 3 independent experiments. (B) CypD depletion decreased the percentage of stationary mitochondria in Aβ-treated neurons. There were no significant changes in the percentage of stationary mitochondria between vehicle-treated nonTg and *Ppif*<sup>-/-</sup> neurons. Data were collected from 1380, 1074, 1410 mitochondria from vehicle, Aβ and rAβ groups in nonTg neurons, and 1634, 1505, 642 mitochondria in *Ppif*<sup>-/-</sup> neurons, respectively, in 4 independent experiments. (C) CypD depletion restored the decrease in the percentage of anterograde mitochondria (C1) and retrograde mitochondria (C2) in Aβ-treated neurons. Data were collected from 4 independent experiments. (D) CypD depletion increased the velocity of mitochondrial movement. (D1) Aβ treatment decreased the velocity of anterograde movement of nonTg mitochondria but not in CypD-deficient (*Ppif*<sup>-/-</sup>) mitochondria. Data were collected from 209, 141, 46 mitochondria from vehicle, Aβ and rAβ groups in nonTg neurons, and 158, 209, 52 mitochondria in *Ppif*<sup>-/-</sup> neurons. (D2–3) The cumulative distribution data showed a left shift of the velocity of anterograde mitochondria when comparing the curve for Aβ-treated nonTg mitochondria to *Ppif*<sup>-/-</sup> mitochondria. Data were collected from 3 independent experiments, respectively. (D4) Aβ treatment had no effect on the velocity of the retrograde mitochondria from both nonTg and *Ppif*<sup>-/-</sup> mice. (E) CypD depletion rescued axonal mitochondrial mobility. Images in the top portion of the panel and kymographs in the lower panel were generated from the live imaging movies. In the kymographs, the X axis represents the mitochondrial position and the Y axis is time. Vertical white lines represent stationary mitochondria and diagonal lines represent moving mitochondria. Anterograde movements are from left to right, retrograde movements are reversed. Scale bars represent 10 μm. doi:10.1371/journal.pone.0054914.g001

vehicle groups (Fig. 2A vehicle:  $1.483 \pm 0.071$  vs. Aβ:  $1.256 \pm 0.043$  μm), the average length of Aβ superimposed *Ppif*<sup>-/-</sup> mitochondria was better preserved than that of Aβ-treated nonTg mitochondria (Fig. 2A–C; *Ppif*<sup>-/-</sup>:  $1.256 \pm 0.043$  μm vs. nonTg:  $0.933 \pm 0.037$  μm). No significant difference was found in an average length when comparing vehicle-treated nonTg to *Ppif*<sup>-/-</sup> axonal mitochondria (Fig. 2A). The rAβ as a control did not alter axonal mitochondrial length (Fig. 2A–C). These results suggest that Aβ toxicity leads to increased axonal mitochondrial fragmentation and importantly, this effect is significantly attenuated by CypD depletion.

### CypD-associated Axonal Calcium Perturbation Alters Axonal Mitochondrial Transport

Aβ has been shown to instigate intra-neuronal calcium elevation [35,36], and the elevated intra-neuronal calcium is known to inhibit mitochondrial transport [37,38]. Given that blockade of CypD-mediated mPTP formation significantly increases mitochondrial calcium buffering capability to maintain intra-cellular calcium homeostasis [12,27], we evaluated whether CypD deficiency protects axonal mitochondrial motility by stabilizing intra-neuronal calcium in Aβ-insulted neurons. First, we measured intra-axonal calcium levels in Aβ-treated neuron as compared with vehicle-treated neurons by quantifying the staining intensity of Fluo-4, a cytoplasmic calcium indicator, and then evaluated the

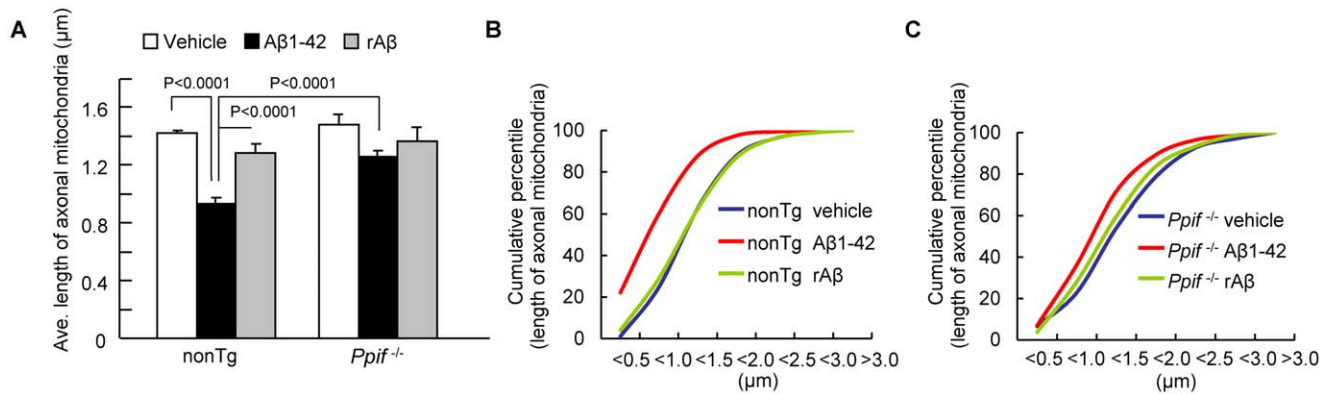


**Figure 2. Effect of CypD on Aβ-induced changes in axonal mitochondrial morphology.** (A) The average length of axonal mitochondria decreased in Aβ-treated nonTg neurons, but was largely preserved in *Ppif*<sup>-/-</sup> neurons. Data were collected from 3 independent experiments. (B, C) Cumulative distribution data showed that Aβ treatment caused a remarkable increase in fragmentation of small mitochondria and a decrease in the numbers of long mitochondria in nonTg neurons; this was partially attenuated in *Ppif*<sup>-/-</sup> neurons. doi:10.1371/journal.pone.0054914.g002

effect of CypD blockade. As shown in **figure 3**, Aβ-treated nonTg axons had a 2.3-fold higher Fluo-4 intensity than vehicle-treated nonTg axons (**Fig. 3A–B1–2**), while axons treated with cyclosporine A (CsA), a pharmacological inhibitor of CypD, (**Fig. 3A–B3**) or genetic CypD-deficient axons (**Fig. 3A–B4–5**) showed no significant change in calcium levels in the presence of Aβ. These results demonstrate that blockade of CypD attenuates Aβ-induced intra-neuronal calcium elevation and maintains intra-neuronal calcium homeostasis.

To further validate the role of CypD blockade on Aβ-induced calcium elevation as shown in Fig. 3A–B on abnormal axonal mitochondrial transport, we evaluated the direct effect of calcium overload on mitochondrial transport. Because CypD deficiency protects cell death from A23187-induced Ca<sup>2+</sup> overload, a strong inducer of calcium elevation in intact cells [27], we assessed the effect of CypD depletion on A23187-mediated alterations in axonal mitochondrial transport. Neurons were exposed to 5 μM Calcium Ionophore (A23187). Axonal mitochondrial transport was recorded pre- and post-treatment with A23187 in the same neurons. Thirty minutes after A23187 treatment, the total of movable nonTg axonal mitochondria decreased by ~50% (**Fig. 3C, 3G1**; 20.02±5.12% in post-treatment vs. 42.54±3.31% in pre-treatment). As a result, the percentage of stationary mitochondria was significantly increased (**Fig. 3D, 3G1**; 57.46±3.31% in pre-treatment vs. 79.98±5.12% in post-treatment). Similarly, A23187 treatment reduced anterograde and retrograde movement of mitochondria by ~54% (**Fig. 3E, 3G1**; 23.73±1.56% in pre-treatment vs. 10.79±4.02% in post-treatment) and ~50% (**Fig. 3F, 3G1**; 18.81±2.18% in pre-treatment vs. 9.23±2.39% in post-treatment), respectively. Notably, *Ppif*<sup>-/-</sup> axonal mitochondria are resistant to A23187-altered mitochondrial movement when evaluated for the percentage of movable vs. stationary mitochondria, anterograde or retrograde movement (**Fig. 3C–G**). These results indicate that calcium imbalance plays a role in axonal mitochondrial trafficking and that CypD depletion protects against calcium-mediated disruption of axonal mitochondrial transport and motility.

#### Effect of CypD Deficiency on ROS-Instigated Alterations in Axonal Mitochondrial Transport

Because mitochondria are a major site of reactive oxygen species (ROS) production and because the formation of CypD-mediated mPTP triggers mitochondrial ROS generation, we next

examined whether increased ROS generation contributes to impaired axonal mitochondrial transport. We first measured intra-axonal ROS levels using 2′7′-dichlorofluorescein diacetate (DCF-DA) fluorescent probe as an indicator of intracellular ROS in Aβ-treated axons for the comparison with vehicle-treated axons. Aβ-treated nonTg neurons revealed significantly higher DCF-DA intensity than the vehicle-treated group (**Fig. 4A, 4B1–2**), while CypD blockade produced by the addition of CsA (**Fig. 4A, 4B3**) or genetic deletion of CypD (**Fig. 4A, 4B4–5**) significantly blunted Aβ-induced increase in axonal DCF-DA intensity. These results indicate that blockade of CypD attenuates axonal ROS production or accumulation following Aβ insults.

To further evaluate whether increased axonal ROS production contributes to Aβ-mediated alterations observed in axonal mitochondrial trafficking, we examined the effects of the antioxidant Probulcol on Aβ-impaired mitochondrial movement. Treatment with Probulcol completely rescued the reduced percentage of movable mitochondria following Aβ treatment (**Fig. 4C–D**; from 26.87±1.59% to 41.53±2.86%). Accordingly, probulcol treatment protected against Aβ-induced disruption of anterograde (from 14.44±1.40% to 21.83±1.28%) and retrograde mitochondrial movement (from 12.23±1.61% to 17.36±1.23%) (**Fig. 4C–D**).

#### CypD-dependent Activation of p38 MAP Kinase Underlies the Axonal Mitochondrial Injury

It is known that Aβ activates a variety of kinases including p38/MAP kinase [39,40] and that impaired mPTP leads to activation of p38 [41]. ROS and calcium are inducers for activation of p38/MAP kinase [42–44]. P38 activation inhibits fast axonal transport (FAT) by phosphorylation of kinesin (motor protein associated with FAT), which are respectively responsible for axonal mitochondrial transport [45,46]. We therefore examined the relatively unexplored role of CypD-dependent mPTP in activation of p38 on Aβ-mediated axonal mitochondrial damage. To do so, we first analyzed the effect of CypD on Aβ-induced phosphorylation of p38 by immunoblotting. As shown in **figure 5A–B**, Aβ-treated nonTg neurons exhibited significantly increased levels of p38 phosphorylation compared to vehicle-treated nonTg neurons (**Fig. 5A**). Addition of a specific p38 inhibitor (SB203580) to neurons completely suppressed p38 phosphorylation (**Fig. 5A**). Interestingly, CypD-deficient neurons were resistant to Aβ-induced p38 phosphorylation (**Fig. 5A–B**). It was noted that the

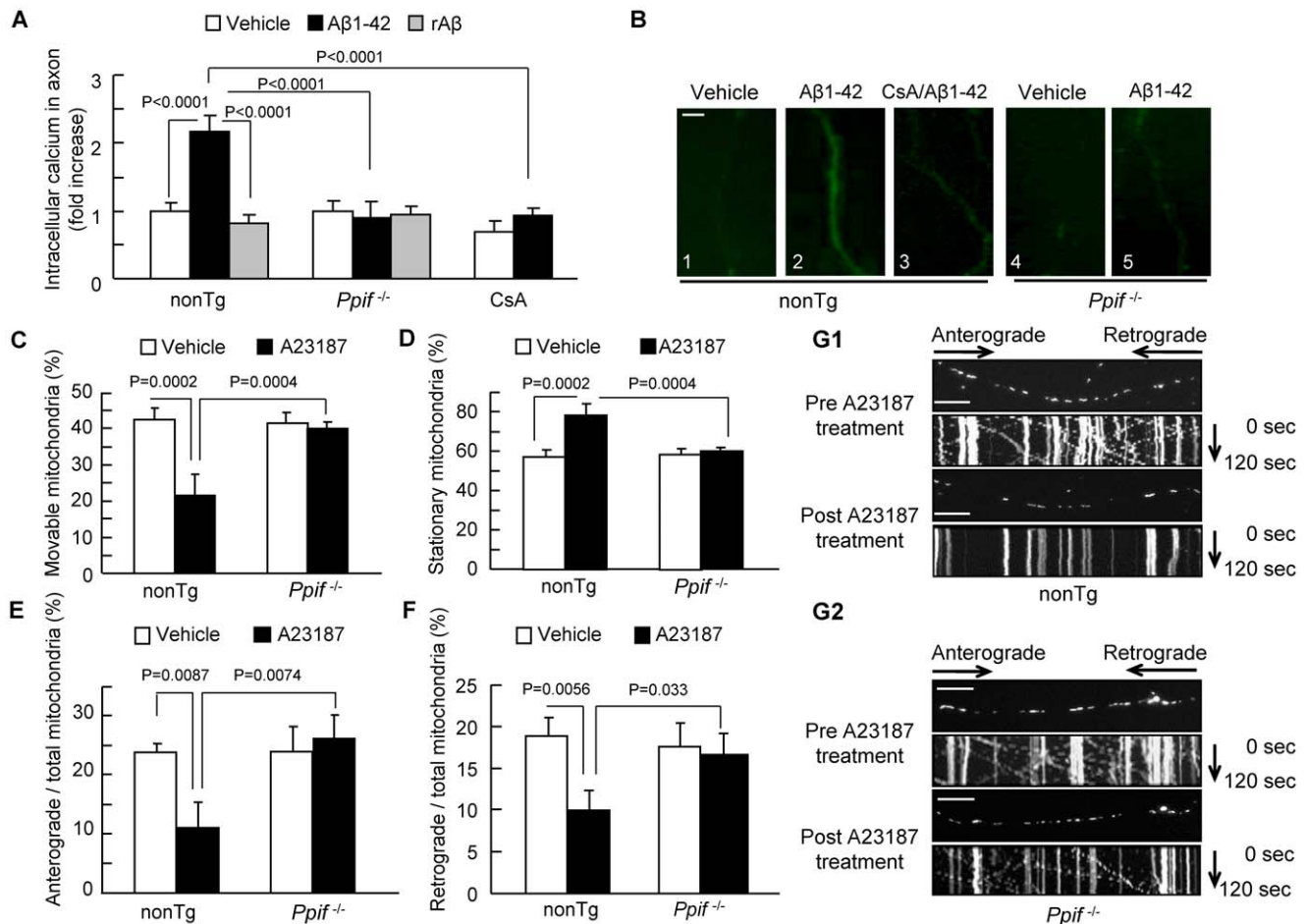


**Figure 3. Effect of CypD depletion on A $\beta$ -induced intra-axonal calcium elevation.** (A) A $\beta$ -treated nonTg hippocampal neurons displayed an increase in axonal calcium levels. CypD-deficient or CsA-treated (500 nM for 24 hours) neurons diminished elevated levels of calcium. rA $\beta$  had no effect on axonal calcium levels. Data were derived from 3 independent experiments. (B) Representative images of axonal calcium staining in nonTg and *Ppif*<sup>-/-</sup> hippocampal neurons at indicated treatment. Scale bar represents 2  $\mu$ m. (C–G2) Effect of CypD depletion on calcium ionophore (A23187)-impaired axonal mitochondrial motility. NonTg and *Ppif*<sup>-/-</sup> hippocampal neurons were exposed to A23187 (5  $\mu$ M for 30 min) and subjected to recording of axonal mitochondrial movements including movable (C), stationary (D), anterograde (E) and retrograde (F) mitochondria. \* $P < 0.05$  vs. other groups of neurons. (G1–G2) The kymograph of axonal mitochondrial movement in nonTg (G1) and *Ppif*<sup>-/-</sup> (G2) neurons before and after A23187 treatment. A23187 treatment resulted in less movement than the vehicle-treated group. *Ppif*<sup>-/-</sup> neurons revealed increased moving traces compared to nonTg neurons in the presence of A23187. Scale bar represents 10  $\mu$ m. doi:10.1371/journal.pone.0054914.g003

baseline of phospho-p38 or total p38 in *Ppif*<sup>-/-</sup> neurons was comparable to that in nonTg neurons, suggesting no effect of CypD deficiency on p38 signal transduction under physiological condition. Based on the observations that CypD depletion significantly stabilized A $\beta$ -induced intracellular calcium and ROS perturbations in neurons and elevated intracellular calcium and ROS are associated with axonal mitochondrial transport and dynamics defects, we then tested whether CypD deficiency inhibits A23187-induced p38 activation by stabilizing intracellular calcium levels and whether A $\beta$ -induced p38 activation is suppressed by antioxidant. We first exposed nonTg and CypD deficient neurons to 5  $\mu$ M A23187. Indeed, A23187 treatment significantly increased phospho-p38 compared to vehicle-treated nonTg neurons (Fig. S2). No significant elevation of p38 phosphorylation was detected in A23187-treated CypD deficient neurons (Fig. S2). Similarly, the co-incubation of Probulon with A $\beta$  significantly suppressed A $\beta$ -induced p38 activation in nonTg neurons (Fig. S3). Taken together, these data suggest the linkage of p38 activation

with mPTP associated intracellular calcium and A $\beta$ -induced ROS disturbances.

To determine if there is a direct link of p38 activation to mitochondrial transport, we assessed the effect of p38 inhibitor on axonal mitochondrial transport following A $\beta$  treatment. Treatment with a specific p38 inhibitor (SB203580) resulted in a significantly higher percentage of movable mitochondria in A $\beta$ -insulted neurons than in neurons without SB203580 treatment (Fig. 5C; 35.34 $\pm$ 2.74% with SB203580 vs. 21.94 $\pm$ 2.95% without SB203580). Similarly, SB203580 treatment protected against A $\beta$ -induced alterations in both anterograde and retrograde mitochondria (Fig. 5C). As the result, SB203580 treatment attenuated A $\beta$ -induced reduction in axonal mitochondrial density (Fig. 5D; 0.199 $\pm$ 0.01/ $\mu$ m with SB203580 vs. 0.283 $\pm$ 0.02/ $\mu$ m without SB203580). These results demonstrate that CypD depletion reduces A $\beta$ -mediated activation of p38 contributing to the impairment of axonal mitochondrial transport.

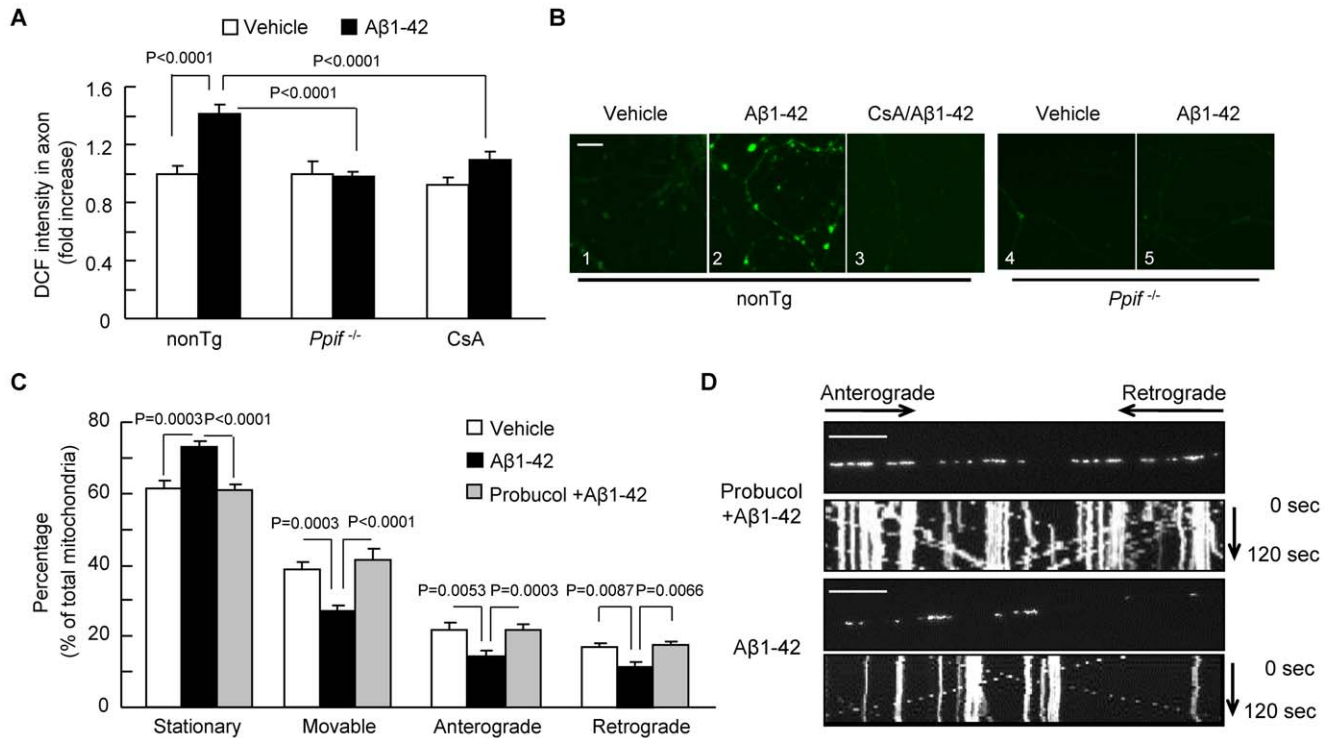


**Figure 4. CypD depletion attenuates Aβ-induced intra-axonal ROS elevation.** (A) Quantification of DCF intensity in nonTg- or *Ppif*<sup>-/-</sup> hippocampal neurons treated with vehicle or Aβ. Addition of CsA (500 nM) to cells for 24 hours reduced the DCF intensity. Data were derived from 3 independent experiments. (B) Representative images of axonal DCF staining in nonTg and *Ppif*<sup>-/-</sup> hippocampal neurons for the indicated treatment. Scale bar is 10 μm. (C–D) Effect of antioxidant (Probecol) on Aβ-induced axonal mitochondrial motility. (C) Administration of Probecol (5 μM, 24 hours) ameliorated changes in Aβ-induced axonal mitochondrial motility. (D) Kymograph images show the protected effects of axonal mitochondrial moving traces following Probecol treatment. Scale bar is 10 μm. doi:10.1371/journal.pone.0054914.g004

### CypD Depletion Protects Against Aβ-induced Synaptic Damage

To analyze the contribution of abnormal axonal mitochondrial transport and/or its directionality to synaptic dysfunction and loss of synapses in Aβ-rich environment, we measured synaptic activity by recording the spontaneous miniature excitatory post-synaptic currents (mEPSCs) and also quantified synaptic density. To determine the effect of CypD on synaptic activity, nonTg and *Ppif*<sup>-/-</sup> neurons were treated with Aβ and then subjected to whole-cell patch-clamp recording of mEPSCs. The frequency of mEPSCs is largely associated with the probability of presynaptic release and the amplitude of mEPSCs at certain levels relies on the size of the vesicle-releasing pool in presynaptic regions [47–49]. Vehicle-treated nonTg and *Ppif*<sup>-/-</sup> neurons showed similar patterns of mEPSCs frequency and amplitude, suggesting no effect of CypD deficiency on the spontaneous nonaction potential-dependent activation of synapses under physiological condition. However, Aβ-insulted nonTg neurons showed a 54.6% decrease in mEPSCs frequency, compared to 16.4% reduction in *Ppif*<sup>-/-</sup> neurons (Fig. 6A). As a result, Aβ-superimposed *Ppif*<sup>-/-</sup> neurons significantly preserved mEPSCs frequency (Fig. 6A, 6C;  $1.84 \pm 0.24$  Hz in *Ppif*<sup>-/-</sup> neurons vs.  $1.09 \pm 0.23$  Hz in nonTg neurons). Similarly, the amplitude of mEPSC was significantly increased in Aβ-treated *Ppif*<sup>-/-</sup> neurons compared to Aβ-treated nonTg neurons (Fig. 6B–C;  $61.88 \pm 3.05$  pA in *Ppif*<sup>-/-</sup> vs.  $47.03 \pm 3.28$  pA in nonTg neurons).

To examine the protective effect of CypD depletion on Aβ-induced loss of synapses, we quantified synaptophysin-positive clusters attaching to dendrites in cultured hippocampal neurons

derived from nonTg and CypD-deficient mice. Synapses were recognized as synaptophysin-positive clusters attaching to dendrites and dendrites were determined by MAP2 (microtubule-associated protein 2) staining. Aβ-treated nonTg neurons exhibited significantly decreased presynaptic density compared to vehicle-treated control (Fig. 6D–E; vehicle:  $0.492 \pm 0.029/\mu\text{m}$  vs Aβ:  $0.273 \pm 0.02/\mu\text{m}$ ), whereas CypD depletion completely reversed the loss of presynaptic density (Fig. 6D–E;  $0.527 \pm 0.026/\mu\text{m}$ ). The rAβ did not affect synaptic density (Fig. 6D–E;  $0.506 \pm 0.019/\mu\text{m}$ ). There was no difference in presynaptic density between nonTg and *Ppif*<sup>-/-</sup> neurons in the vehicle-treated groups (Fig. 6D–E). To determine effect of p38 activation on loss of synapses, neurons were treated with specific p38 inhibitor (SB203580) for 30 min prior to Aβ. As shown in Fig. 6C–D, the addition of SB203580 to culture increased synaptic density (Fig. 6F–G;  $0.442 \pm 0.033\%$  with SB203580 vs.  $0.273 \pm 0.020\%$  without SB203580). Taken together, our results indicate that lack of CypD protects neuron from Aβ-insulted synaptic injury with involvement of CypD/Aβ-associated P38 MAPK signaling, which is associated with compromised mitochondrial transport in axon.

### Discussion

Abnormal axonal mitochondrial transport is a recently recognized mitochondrial pathology induced by Aβ [20–26,50]. The precise mechanisms underlying impairments in axonal mitochondrial transport and the link of mitochondrial dysfunction to synaptic damage in AD are not well understood. In this study, we

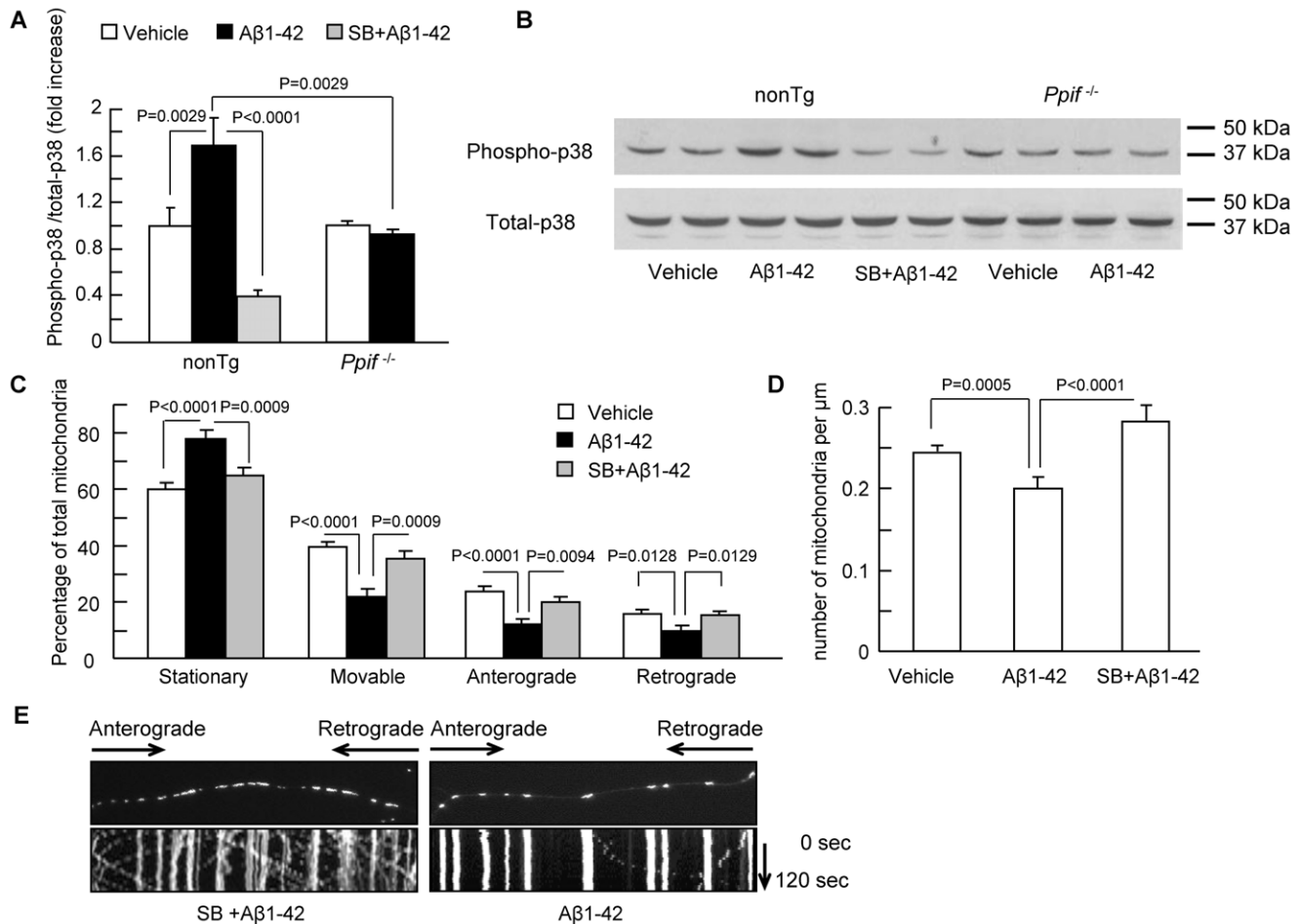


**Figure 5. Effect of CypD on Aβ-induced activation of p38 MAP kinase and axonal mitochondrial motility.** (A) Quantification of phospho-p38 immunoreactive bands (pT180/pY182) in hippocampal neurons treated with vehicle, Aβ, or SB203580 (SB, 1 μM) plus Aβ, respectively, which was normalized for the total p38. (B) Representative immunoblots for phospho- and total-p38. (C–E) Administration of p38 inhibitor, SB203580 (1 μM, 24 hours) to cells ameliorated Aβ-induced axonal mitochondrial motility changes (C) and mitochondrial density (D). (E) Kymographs showed the protected effects of axonal mitochondrial movement after SB203580 treatment. Scale bar is 10 μm. doi:10.1371/journal.pone.0054914.g005

analyzed the effect of CypD on Aβ-mediated mitochondrial motility and distribution in hippocampal neurons using mice with genetic depletion of CypD. Our results show that CypD depletion protects against Aβ-induced alterations in axonal mitochondrial transport as shown by increased mitochondrial motility and distribution, and improved anterograde and retrograde movement. The possible mechanisms underlying the protective effect of lacking CypD are suppressed mPTP opening, reduced ROS production, and increased calcium buffering capacity in axonal mitochondria. Furthermore, we also demonstrated that CypD-mediated p38 activation contributes to Aβ-impaired axonal mitochondrial transport and synaptic injury. We focus our attention on the protective effect of CypD deficiency on axonal mitochondrial movement in view of the essential role of normal axonal mitochondrial trafficking in supporting synaptic plasticity. Our current study uncovers the role of CypD in Aβ-mediated alterations in axonal mitochondrial motility and dynamics contributing to synaptic degeneration in AD.

An increasing body of evidence suggests that oligomeric Aβ inhibits axonal mitochondrial transport and breaks the mitochondrial fusion/fission balance. Aβ-disrupted axonal mitochondrial trafficking is a mechanism underlying synaptic degeneration in AD

[20,23–26,50]. In the present of study, we examined the effect of relatively low concentration of Aβ (200 nM) that did not alter cell viability on axonal mitochondrial transport to mimic low *in vivo* levels and chronic Aβ insults in AD brain. Similar to what have been reported [20,23–26,50], under our experimental condition, 200 nM oligomeric Aβ significantly reduced mitochondrial density and movement in axon by 30–40% (Fig. 1A–D and 2A) without significant changes in the cell viability. This suggests an early change in axonal mitochondrial trafficking is prior to neuronal death. A relatively low concentration of Aβ (200 nM) used in our study may account for the modest effects on mitochondrial movement without significant neurotoxicity. Indeed, a study has shown that the acute treatment of monomeric Aβ demonstrated significant inhibitory effect on neuronal mitochondrial movement [51], suggesting that both Aβ species (monomeric or oligomeric forms) are toxic to neuronal mitochondrial transport. In consideration of the significance of oligomeric Aβ-induced mitochondrial and synaptic dysfunction relevant to the AD pathogenesis [52] and our experimental condition (chronic treatment of low concentration of 200 nM Aβ for 24 hours) in which condition that monomeric Aβ is prone to form oligomers during incubation time [53], we used oligomeric Aβ for all our experiments. In addition,

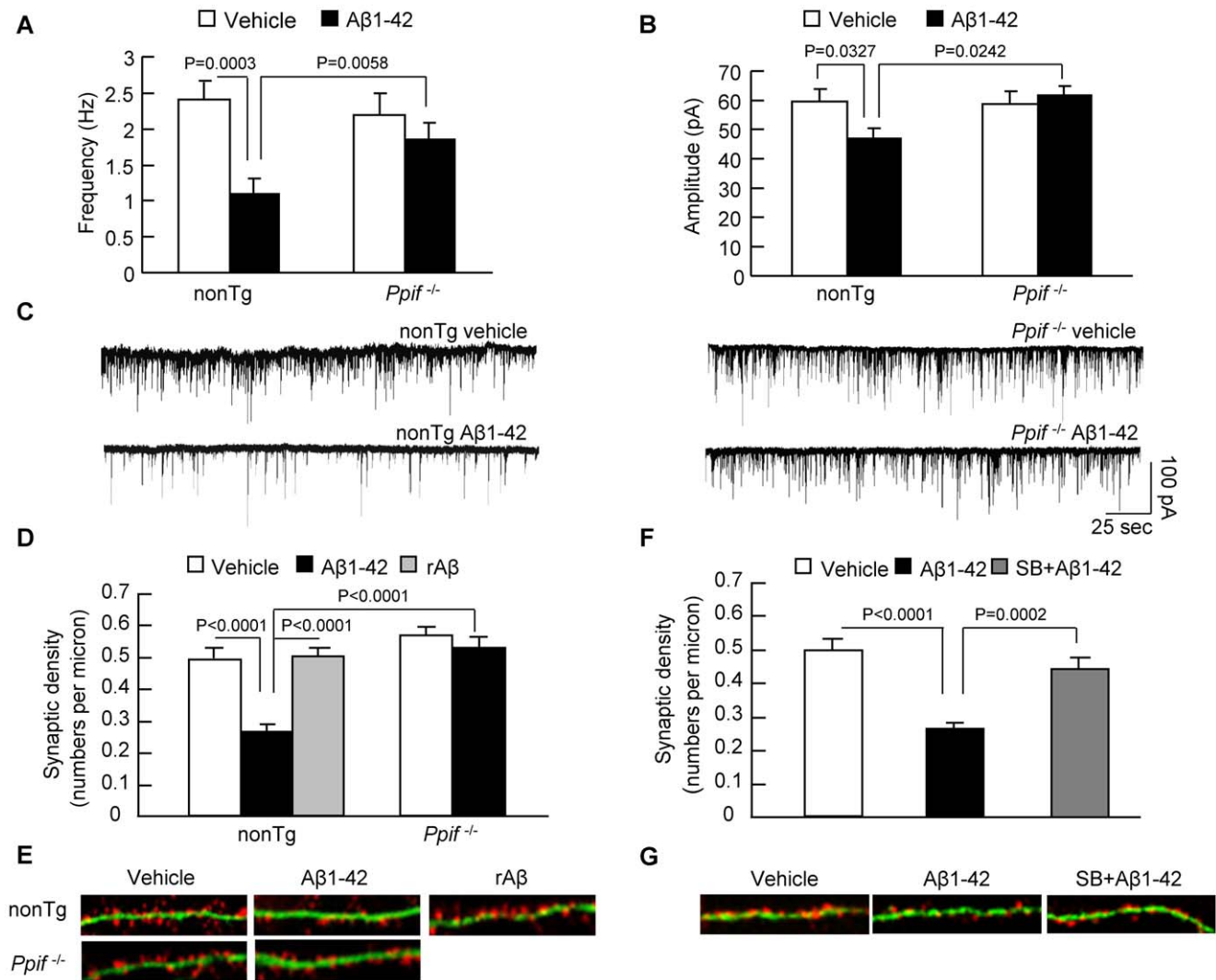


**Figure 6. Effect of CypD on Aβ-induced synaptic damage.** (A–C) Electrophysiological recording of mEPSCs for Aβ-treated nonTg and *Ppif*<sup>-/-</sup> neurons. CypD deficiency alleviated Aβ-induced decrease in mEPSCs frequency (A) and amplitude (B). Data were derived from 16–19 neurons for each group. (C) Representative traces of mEPSCs in the indicated group. Scale bar represents 100 pA in amplitude and 25 seconds in time. (D–E) Effect of CypD deficiency on synaptic density. The results were derived from 20–30 neurons of each group. Dendrites were visualized by the staining of MAP2 and synapses were recognized as synaptophysin-positive clusters overlapping with dendrites. (E) Representative images for double staining of synaptophysin and MAP-2 in the indicated groups. MAP2 is shown in green color and synaptophysin is labeled by red fluorescence. (F–G) Effect of Aβ-induced activation of p38 MAP kinase on synaptic density. (F) Administration of p38 inhibitor, SB203580 (1 μM, 24 hours) to cells ameliorated Aβ-induced synaptic loss. (G) Representative images showed the protected effects of synaptic density after SB203580 treatment. doi:10.1371/journal.pone.0054914.g006

reversed Aβ peptide (rAβ) that has the same molecular weight and composition of amino acids with Aβ but without biological effects was used as a widely accepted control to verify the specific effects of Aβ [54,55].

To elucidate the protective mechanisms of CypD depletion, we focused on the major consequences of mPTP formation on axonal mitochondrial motility and morphology: impaired mitochondrial calcium handling capacity and ROS generation. Aβ has been reported to increase intracellular Ca<sup>2+</sup>, which could have more targets than mitochondrial trafficking. In view of the role of CypD-dependent mPTP on maintaining intracellular Ca<sup>2+</sup> homeostasis, significance of Aβ-impaired mitochondrial transport on synaptic degeneration, and unexplored role of CypD on mitochondrial transport, it is essential and logical to investigate the involvement of CypD on Aβ-induced abnormal axonal mitochondrial transport. CypD is a key component for the formation of mPTP

contributing to maintaining calcium homeostasis. CypD deficiency inhibits opening of mPTP, subsequently, increases mitochondrial calcium buffering capacity in response to changes in intracellular calcium levels such as calcium overloading [12,27,29,56]. Therefore, CypD-dependent mPTP is an important regulating mechanism of intracellular Ca<sup>2+</sup> homeostasis.

We have presented data showing that blockade of CypD by genetic depletion of CypD or pharmacological CypD inhibitor significantly suppressed Aβ-induced elevation of the intracellular calcium in axon (Fig. 3A), which are consistent with our [12] and other [27] published studies. These results suggest that an inhibitory effect of CypD deficiency on Aβ-mediated changes in intracellular Ca<sup>2+</sup> levels is important for maintaining normal mitochondrial transport. To test this hypothesis, we examined a direct effect of CypD deficiency on ionomycin (A23187)-induced Ca<sup>2+</sup> overload, a strong inducer of Ca<sup>2+</sup> elevation in intact cells,

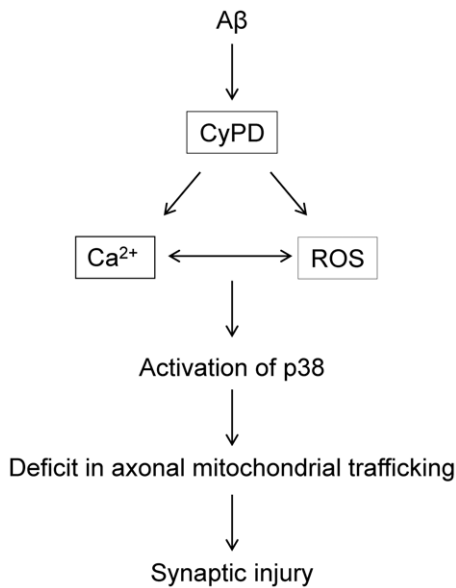


**Figure 7. Working hypothesis.** A $\beta$ -Cyclophilin D mediates impairments in axonal mitochondrial transport. In the presence of A $\beta$ , there is an increase in the opening of CypD-mediated mitochondrial permeability transition pore (mPTP), leading to disruption of Ca<sup>2+</sup> balance and increase in reactive oxygen species (ROS) production/accumulation. Consequently, elevation of Ca<sup>2+</sup> and oxidative stress activates downstream signal pathway p38 MAP Kinase contributing to mitochondrial dysfunction, deficits in axonal mitochondrial trafficking, eventually, synaptic damage.  
doi:10.1371/journal.pone.0054914.g007

and alterations in axonal mitochondrial transport [27]. As expected, CypD-deficient neurons blocked A23187-induced elevation of intracellular Ca<sup>2+</sup> (Fig. S4) and p38 activation (Fig. S2). This could be a mechanism of the protective effect of CypD deficiency on A23187-altered axonal mitochondrial trafficking (Fig. 3C–G). Compared to the effect of A $\beta$ , A23187 treatment had a greater effect on mitochondrial transport (50% decline in A23187 treatment vs. 30–40% in A $\beta$ -treated cells). A strong induction of calcium elevation in intact cells (high levels of Ca<sup>2+</sup>) by A23187 could be the explanation for a more dramatic effect of A23187 (50% in Fig. 3C, E–F) than A $\beta$  treatment (30% in Fig. 1A–B, C2, D1 and 40% in Fig. 2A–C) in which elevated levels of Ca<sup>2+</sup> are expected to be lower than A23187-treated cells. A direct role of intracellular calcium in controlling axonal mitochondrial motility and dynamics is also supported by the recent study. For example, calcium-induced mitochondrial dissociation has been postulated as a potential mechanism for modulation of mitochondrial docking under physiological conditions [57]. Increased calcium levels are reported to decrease mitochondrial movement/transport by interrupting Miro and kinesin complexes [57,58]. At pathological states with significant and sustained calcium elevation achieved by the activation of N-Methyl-D-aspartate (NMDA) receptors [37] or the application of A23187 [59], mitochondrial morphology and movement are substantially disrupted, suggesting the impact of pathological intracellular calcium perturbations. In A $\beta$ -rich environment where calcium levels are abnormally high [60–63], increased mitochondrial detachments occur in A $\beta$ -treated axons (represented by an increased percentage of stationary mitochondria). Thus, axonal mitochondria are crucial to the calcium buffering process. Maintenance of axonal calcium homeostasis by CypD depletion is an underlying mechanism for controlling axonal mitochondrial

calcium in the face of A $\beta$  insults. A $\beta$ -mediated elevation of calcium is a potential mechanism at the nexus of A $\beta$  toxicity and alterations in mitochondrial motility. The dramatic protection of lacking CypD against A23187-disturbed calcium balance as well as mitochondrial motility and dynamics changes provides substantial evidence that the blockade of CypD-mediated mPTP counteracts calcium-instigated axonal mitochondrial alterations in trafficking and morphology.

Another major consequence of CypD-mediated mPTP formation is increased ROS production/accumulation leading to release of ROS from mitochondrial to cytosol. As Ca<sup>2+</sup> metabolism and oxidative stress are intertwined, especially in mitochondrial processes, these organelles can become severely dysfunctional during the permeability transition in combination with effects of oxidative stress and dysregulation of cytosolic free Ca<sup>2+</sup>. Indeed, in the present study, we report reduced mitochondrial calcium buffering capacity, increased membrane permeability transition, and accumulation of ROS in axons in the presence of A $\beta$ . ROS has been implicated in disruption of mitochondrial movement. For example, zinc-induced ROS generation is associated with phosphatidylinositol (PI) 3-kinase activation, which in turn disrupts mitochondrial transport in neurons [64]. However, to our knowledge, the contribution of axonal ROS dysregulation to A $\beta$ -induced defects in mitochondrial transport has not yet been documented. We showed here that the addition of probucol, an antioxidant drug to suppress ROS generation, or genetic deletion of CypD to blunt oxidative stress and to enhance mitochondrial calcium buffer capability significantly rescues mitochondrial movement against A $\beta$  toxicity, indicating the significance of oxidative stress on A $\beta$ -altered axonal mitochondrial trafficking. These data support that A $\beta$ -induced intra-axonal ROS has deleterious effects on transport.

Activation of P38 mitogen-activated protein kinase (MAPK) is associated with increased intracellular calcium, ROS production/accumulation, A $\beta$  stimulation, and mitochondrial stress [43,65–71]. We demonstrated that levels of P38 phosphorylation were significantly increased in A $\beta$ -treated neurons. Antioxidant Probucol blocked A $\beta$ -induced p38 activation, indicating a role of A $\beta$ -induced oxidative stress in disruption of signal transduction such as p38 MAP kinase contributing to abnormal axonal mitochondrial transport. Notably, A $\beta$ -induced p38 phosphorylation was blunted in neurons lacking CypD. The addition of a specific p38 inhibitor (SB203580) resulted in pronounced preservation of mitochondrial motility and morphology even in the face of A $\beta$  insults, indicating the involvement of CypD/A $\beta$ -associated p38 MAPK signaling in disruption of axonal mitochondrial trafficking. The application of p38 inhibitor did not interfere with A $\beta$ -induced calcium elevation (data not shown). These results suggest that p38 is a downstream target of A $\beta$ . Thus, we propose that CypD-dependent impaired calcium homeostasis and ROS production/accumulation in axons are responsible for p38 MAPK activation, which leads to further mitochondrial injury including abnormal axonal mitochondrial transport and loss of synapse. The detailed mechanisms of P38 activation in injuring axonal mitochondrial transport need further investigation. For example, P38 activation is connected with changes in mitochondrial movement via phosphorylation of kinesin [46] and dynein [72], which dissociates mitochondria from the motor proteins. In addition to p38, perturbations of several other signaling cascades including PKA [51] and GSK-3 $\beta$  [23] are also reported to be involved in A $\beta$ -induced disruption in mitochondrial transport. Given the tight interaction of these signaling cascades [73], they may work together in keeping axonal mitochondrial movement in normal fashion while their independent effects on mitochondrial trafficking remain unclear. In view

of potential involvement of motor proteins in mitochondrial movement, we will further examine whether mPTP-associated axonal mitochondrial transport changes are related to changes of motor proteins such as hyperphosphorylation of dynein and kinesin and altered Miro activity state in near future. Nevertheless, our study suggests that CypD-involved activation of p38 signaling plays a role, at least in part, in A $\beta$ -insulted abnormal mitochondrial transport in axon.

Axonal mitochondria are dynamic organelles and their trafficking and docking are critical for synaptic plasticity and function. Synaptic loss and deactivation are biological basis of AD. Increasing evidence emphasizes the importance of mitochondria for the maintenance of synaptic function. Defects in dendritic mitochondria lead to dendritic degeneration [74] and injured mitochondria in the presynapse region are associated with compromised presynaptic function [75]. Mitochondrial transport maintains functional mitochondria around synapses [76]. Previously, we and other groups showed that A $\beta$  insults results in impaired mitochondrial distribution and trafficking in axons [20,23–26], while in the present study, we demonstrate the protective effects of CypD depletion on A $\beta$ -mediated deficits in axonal mitochondrial transport and synaptic injury including synaptic activity and loss of synapses. Notably, blockade of p38 activation significantly rescue synaptic loss insulted by A $\beta$  (Fig. 6F–G), supporting a connection of CypD/A $\beta$ -involved signal transduction (p38) with mitochondrial and synaptic degeneration.

In summary, our data offer new insights into the mechanism of mitochondrial perturbation in the pathogenesis of AD, specifically the role of CypD in axonal mitochondrial transport. A $\beta$ -CypD interaction promotes opening of mitochondrial permeability transition pore, consequently, disrupts calcium balance and enhances production/accumulation of ROS, thereby further activating P38 MAPK signal transduction pathway. All these events disrupt mitochondrial trafficking and dynamics, ultimately causing synaptic damage (Fig. 7). We have clearly demonstrated that CypD depletion protects axonal mitochondrial transport from A $\beta$  insults along with suppressing A $\beta$ -induced elevation of calcium and accumulation of oxidative stress. Importantly, CypD depletion also suppressed A $\beta$ -induced activation of p38/MAPK and this inhibition rescued axonal mitochondrial movement and pre-synaptic density. Thus, our results provide evidence that CypD/A $\beta$ -mediated mitochondrial dysfunction is correlated with disruption of axonal mitochondrial transport and synaptic injury. These findings significantly enhance our understanding of the pathological role of CypD in axonal pathology in AD.

## References

- Kang JS, Tian JH, Pan PY, Zald P, Li C, et al. (2008) Docking of axonal mitochondria by syntrophin controls their mobility and affects short-term facilitation. *Cell* 132: 137–148.
- Miller KE, Sheetz MP (2004) Axonal mitochondrial transport and potential are correlated. *Journal of cell science* 117: 2791–2804.
- Billups B, Forsythe ID (2002) Presynaptic mitochondrial calcium sequestration influences transmission at mammalian central synapses. *The Journal of neuroscience : the official journal of the Society for Neuroscience* 22: 5840–5847.
- David G, Barrett EF (2000) Stimulation-evoked increases in cytosolic [Ca<sup>2+</sup>] in mouse motor nerve terminals are limited by mitochondrial uptake and are temperature-dependent. *The Journal of neuroscience : the official journal of the Society for Neuroscience* 20: 7290–7296.
- Talbot JD, David G, Barrett EF (2003) Inhibition of mitochondrial Ca<sup>2+</sup> uptake affects phasic release from motor terminals differently depending on external [Ca<sup>2+</sup>]. *Journal of neurophysiology* 90: 491–502.
- Chada SR, Hollenbeck PJ (2003) Mitochondrial movement and positioning in axons: the role of growth factor signaling. *The Journal of experimental biology* 206: 1985–1992.
- Chada SR, Hollenbeck PJ (2004) Nerve growth factor signaling regulates motility and docking of axonal mitochondria. *Current biology : CB* 14: 1272–1276.
- Morris RL, Hollenbeck PJ (1993) The regulation of bidirectional mitochondrial transport is coordinated with axonal outgrowth. *Journal of cell science* 104 (Pt 3): 917–927.
- Chang DT, Honick AS, Reynolds IJ (2006) Mitochondrial trafficking to synapses in cultured primary cortical neurons. *The Journal of neuroscience : the official journal of the Society for Neuroscience* 26: 7035–7045.
- Baloh RH, Schmidt RE, Pestronk A, Milbrandt J (2007) Altered axonal mitochondrial transport in the pathogenesis of Charcot-Marie-Tooth disease from mitofusin 2 mutations. *The Journal of neuroscience : the official journal of the Society for Neuroscience* 27: 422–430.
- Caspersen C, Wang N, Yao J, Sosunov A, Chen X, et al. (2005) Mitochondrial Abeta: a potential focal point for neuronal metabolic dysfunction in Alzheimer's disease. *FASEB journal : official publication of the Federation of American Societies for Experimental Biology* 19: 2040–2041.
- Du H, Guo L, Fang F, Chen D, Sosunov AA, et al. (2008) Cyclophilin D deficiency attenuates mitochondrial and neuronal perturbation and ameliorates learning and memory in Alzheimer's disease. *Nature medicine* 14: 1097–1105.

## Supporting Information

**Figure S1** Cultured hippocampal neurons were transfected with pDsRedmito and observed under microscope. The figure showed the image of a transfected neuron. Middle part of the axon (in the frame) was selected for the experiment to detect mitochondrial movement.

(TIF)

**Figure S2** CypD depletion suppresses A23187-induced p38 phosphorylation. NonTg and CypD deficient hippocampal neurons were exposed to 5  $\mu$ M A23187 for 15 and 30 min, respectively. Cell lysates were subjected to immunoblots for phospho- and total-p38. The treatment of A23187 on nonTg neurons significantly increased p38 phosphorylation level as compared to the vehicle-treated neurons (vehicle:  $1 \pm 0.021$  vs. A23187 15 min:  $1.89 \pm 0.047$ ; vehicle vs. A23187 30 min:  $2.06 \pm 0.18$ ). CypD depletion significantly suppressed A23187-induced elevation of phospho-p38. Data were derived from 4 independent experiments.

(TIF)

**Figure S3** Addition of Probuco attenuates A $\beta$ -induced p38 phosphorylation in nonTg neurons. nonTg neurons were treated with A $\beta$  co-incubated in the presence or absence of Probuco (5  $\mu$ M, 24 hours). A $\beta$  treatment resulted in a significant elevation of p38 phosphorylation level as compared to vehicle treatment (vehicle:  $1 \pm 0.077$  vs. A $\beta$ :  $3.06 \pm 0.27$ ), while A $\beta$ -induced p38 phosphorylation was inhibited by the addition of Probuco (A $\beta$ :  $3.06 \pm 0.27$  vs. A $\beta$ +Probuco:  $1.15 \pm 0.46$ ). Data were derived from 3 independent experiments.

(TIF)

**Figure S4** Effect of CypD depletion on A23187-induced intra-axonal calcium elevation. NonTg and *Ppif*<sup>-/-</sup> hippocampal neurons were exposed to A23187 (5  $\mu$ M for 30 min) and subjected to recording of intra-axonal calcium before and after A23187 treatment. A23187 treatment resulted in increased axonal calcium level in nonTg neurons. *Ppif*<sup>-/-</sup> neurons abolished A23187-induced calcium elevation.

(TIF)

## Author Contributions

Conceived and designed the experiments: SSS JXC LG HD. Performed the experiments: LG HD SQY XPW. Analyzed the data: LG HD SQY XPW. Contributed reagents/materials/analysis tools: LG HD SQY XPW GMM. Wrote the paper: SSS LG HD.

13. Du H, Yan SS (2010) Mitochondrial permeability transition pore in Alzheimer's disease: cyclophilin D and amyloid beta. *Biochimica et biophysica acta* 1802: 198–204.
14. Hansson MJ, Mansson R, Morota S, Uchino H, Kallur T, et al. (2008) Calcium-induced generation of reactive oxygen species in brain mitochondria is mediated by permeability transition. *Free radical biology & medicine* 45: 284–294.
15. Lustbader JW, Cirilli M, Lin C, Xu HW, Takuma K, et al. (2004) ABAD directly links Abeta to mitochondrial toxicity in Alzheimer's disease. *Science* 304: 448–452.
16. Manczak M, Anekonda TS, Henson E, Park BS, Quinn J, et al. (2006) Mitochondria are a direct site of A beta accumulation in Alzheimer's disease neurons: implications for free radical generation and oxidative damage in disease progression. *Human molecular genetics* 15: 1437–1449.
17. Takuma K, Fang F, Zhang W, Yan S, Fukuzaki E, et al. (2009) RAGE-mediated signaling contributes to intraneuronal transport of amyloid-beta and neuronal dysfunction. *Proceedings of the National Academy of Sciences of the United States of America* 106: 20021–20026.
18. Yao J, Irwin RW, Zhao L, Nilsen J, Hamilton RT, et al. (2009) Mitochondrial bioenergetic deficit precedes Alzheimer's pathology in female mouse model of Alzheimer's disease. *Proceedings of the National Academy of Sciences of the United States of America* 106: 14670–14675.
19. Mao P, Manczak M, Calkins MJ, Truong Q, Reddy TP, et al. (2012) Mitochondria-targeted catalase reduces abnormal APP processing, amyloid beta production and BACE1 in a mouse model of Alzheimer's disease: implications for neuroprotection and lifespan extension. *Hum Mol Genet*.
20. Du H, Guo L, Yan S, Sosunov AA, McKhann GM, et al. (2010) Early deficits in synaptic mitochondria in an Alzheimer's disease mouse model. *Proceedings of the National Academy of Sciences of the United States of America* 107: 18670–18675.
21. Du H, Guo L, Yan SS (2012) Synaptic mitochondrial pathology in Alzheimer's disease. *Antioxid Redox Signal* 16: 1467–1475.
22. Reddy PH, Tripathi R, Truong Q, Tirumala K, Reddy TP, et al. (2012) Abnormal mitochondrial dynamics and synaptic degeneration as early events in Alzheimer's disease: Implications to mitochondria-targeted antioxidant therapeutics. *Biochim Biophys Acta* 1822: 639–649.
23. Decker H, Lo KY, Unger SM, Ferreira ST, Silverman MA (2010) Amyloid-beta peptide oligomers disrupt axonal transport through an NMDA receptor-dependent mechanism that is mediated by glycogen synthase kinase 3beta in primary cultured hippocampal neurons. *The Journal of neuroscience : the official journal of the Society for Neuroscience* 30: 9166–9171.
24. Calkins MJ, Manczak M, Mao P, Shirendeb U, Reddy PH (2011) Impaired mitochondrial biogenesis, defective axonal transport of mitochondria, abnormal mitochondrial dynamics and synaptic degeneration in a mouse model of Alzheimer's disease. *Human molecular genetics* 20: 4515–4529.
25. Calkins MJ, Reddy PH (2011) Amyloid beta impairs mitochondrial anterograde transport and degenerates synapses in Alzheimer's disease neurons. *Biochimica et biophysica acta* 1812: 507–513.
26. Wang X, Perry G, Smith MA, Zhu X (2010) Amyloid-beta-derived diffusible ligands cause impaired axonal transport of mitochondria in neurons. *Neurodegenerative diseases* 7: 56–59.
27. Baines CP, Kaiser RA, Purcell NH, Blair NS, Osinska H, et al. (2005) Loss of cyclophilin D reveals a critical role for mitochondrial permeability transition in cell death. *Nature* 434: 658–662.
28. Baines CP (2007) The mitochondrial permeability transition pore as a target of cardioprotective signaling. *American journal of physiology Heart and circulatory physiology* 293: H903–904.
29. Du H, Guo L, Zhang W, Ryzewska M, Yan S (2011) Cyclophilin D deficiency improves mitochondrial function and learning/memory in aging Alzheimer disease mouse model. *Neurobiology of aging* 32: 398–406.
30. Banker GA, Cowan WM (1979) Further observations on hippocampal neurons in dispersed cell culture. *J Comp Neurol* 187: 469–493.
31. Cai Q, Gerwin C, Sheng ZH (2005) Syntabulin-mediated anterograde transport of mitochondria along neuronal processes. *The Journal of cell biology* 170: 959–969.
32. Oliva AA, Jr., Atkins CM, Copenagle L, Banker GA (2006) Activated c-Jun N-terminal kinase is required for axon formation. *The Journal of neuroscience : the official journal of the Society for Neuroscience* 26: 9462–9470.
33. Sharma G, Vijayaraghavan S (2003) Modulation of presynaptic store calcium induces release of glutamate and postsynaptic firing. *Neuron* 38: 929–939.
34. Trinchese F, Liu S, Ninan I, Puzzo D, Jacob JP, et al. (2004) Cell cultures from animal models of Alzheimer's disease as a tool for faster screening and testing of drug efficacy. *J Mol Neurosci* 24: 15–21.
35. Mattson MP, Cheng B, Davis D, Bryant K, Lieberburg I, et al. (1992) beta-Amyloid peptides destabilize calcium homeostasis and render human cortical neurons vulnerable to excitotoxicity. *The Journal of neuroscience : the official journal of the Society for Neuroscience* 12: 376–389.
36. Ferreira IL, Bajouco LM, Mota SI, Auberson YP, Oliveira CR, et al. (2011) Amyloid beta peptide 1–42 disturbs intracellular calcium homeostasis through activation of GluN2B-containing N-methyl-D-aspartate receptors in cortical cultures. *Cell calcium*.
37. Rintoul GL, Filiano AJ, Brocard JB, Kress GJ, Reynolds IJ (2003) Glutamate decreases mitochondrial size and movement in primary forebrain neurons. *The Journal of neuroscience : the official journal of the Society for Neuroscience* 23: 7881–7888.
38. Yi M, Weaver D, Hajnoczky G (2004) Control of mitochondrial motility and distribution by the calcium signal: a homeostatic circuit. *The Journal of cell biology* 167: 661–672.
39. Origlia N, Bonadonna C, Rosellini A, Leznik E, Arancio O, et al. (2010) Microglial receptor for advanced glycation end product-dependent signal pathway drives beta-amyloid-induced synaptic depression and long-term depression impairment in entorhinal cortex. *The Journal of neuroscience : the official journal of the Society for Neuroscience* 30: 11414–11425.
40. Zhu X, Mei M, Lee HG, Wang Y, Han J, et al. (2005) P38 activation mediates amyloid-beta cytotoxicity. *Neurochemical research* 30: 791–796.
41. Tomasello F, Messina A, Lartigue L, Schembri L, Medina C, et al. (2009) Outer membrane VDAC1 controls permeability transition of the inner mitochondrial membrane in cellulo during stress-induced apoptosis. *Cell research* 19: 1363–1376.
42. Matsuyama D, Kawahara K (2011) Oxidative stress-induced formation of a positive-feedback loop for the sustained activation of p38 MAPK leading to the loss of cell division in cardiomyocytes soon after birth. *Basic research in cardiology* 106: 815–828.
43. Lee MW, Park SC, Yang YG, Yim SO, Chae HS, et al. (2002) The involvement of reactive oxygen species (ROS) and p38 mitogen-activated protein (MAP) kinase in TRAIL/Apo2L-induced apoptosis. *FEBS letters* 512: 313–318.
44. Wright DC, Geiger PC, Han DH, Jones TE, Holloszy JO (2007) Calcium induces increases in peroxisome proliferator-activated receptor gamma coactivator-1alpha and mitochondrial biogenesis by a pathway leading to p38 mitogen-activated protein kinase activation. *The Journal of biological chemistry* 282: 18793–18799.
45. Morfini G, Pignino G, Szebenyi G, You Y, Pollema S, et al. (2006) JNK mediates pathogenic effects of polyglutamine-expanded androgen receptor on fast axonal transport. *Nature neuroscience* 9: 907–916.
46. De Vos K, Severin F, Van Herreweghe F, Vancompernelle K, Goossens V, et al. (2000) Tumor necrosis factor induces hyperphosphorylation of kinesin light chain and inhibits kinesin-mediated transport of mitochondria. *The Journal of cell biology* 149: 1207–1214.
47. Kimura A, Pavlides C (2000) Long-term potentiation/depotentialization are accompanied by complex changes in spontaneous unit activity in the hippocampus. *J Neurophysiol* 84: 1894–1906.
48. Zhang J, Yang Y, Li H, Cao J, Xu L (2005) Amplitude/frequency of spontaneous mEPSC correlates to the degree of long-term depression in the CA1 region of the hippocampal slice. *Brain Res* 1050: 110–117.
49. Rohrbough J, Spitzer NC (1999) Ca(2+)-permeable AMPA receptors and spontaneous presynaptic transmitter release at developing excitatory spinal synapses. *J Neurosci* 19: 8528–8541.
50. Pignino G, Morfini G, Atagi Y, Deshpande A, Yu C, et al. (2009) Disruption of fast axonal transport is a pathogenic mechanism for intraneuronal amyloid beta. *Proceedings of the National Academy of Sciences of the United States of America* 106: 5907–5912.
51. Rui Y, Tiwari P, Xie Z, Zheng JQ (2006) Acute impairment of mitochondrial trafficking by beta-amyloid peptides in hippocampal neurons. *The Journal of neuroscience : the official journal of the Society for Neuroscience* 26: 10480–10487.
52. Benilova I, Karran E, De Strooper B (2012) The toxic Abeta oligomer and Alzheimer's disease: an emperor in need of clothes. *Nature neuroscience* 15: 349–357.
53. Stine WB, Jr., Dahlgren KN, Kraft GA, LaDu MJ (2003) In vitro characterization of conditions for amyloid-beta peptide oligomerization and fibrillogenesis. *The Journal of biological chemistry* 278: 11612–11622.
54. Parameshwaran K, Sims C, Kanju P, Vaithianathan T, Shonsey BC, et al. (2007) Amyloid beta-peptide Abeta(1–42) but not Abeta(1–40) attenuates synaptic AMPA receptor function. *Synapse* 61: 367–374.
55. Perez JL, Carrero I, Gonzalo P, Arevalo-Serrano J, Sanz-Anquela JM, et al. (2010) Soluble oligomeric forms of beta-amyloid (Abeta) peptide stimulate Abeta production via astrogliosis in the rat brain. *Experimental neurology* 223: 410–421.
56. Nakagawa T, Shimizu S, Watanabe T, Yamaguchi O, Otsu K, et al. (2005) Cyclophilin D-dependent mitochondrial permeability transition regulates some necrotic but not apoptotic cell death. *Nature* 434: 652–658.
57. Macaskill AF, Rinholm JE, Twelvetrees AE, Arancibia-Carcamo IL, Muir J, et al. (2009) Miro1 is a calcium sensor for glutamate receptor-dependent localization of mitochondria at synapses. *Neuron* 61: 541–555.
58. Wang X, Schwarz TL (2009) The mechanism of Ca2+ -dependent regulation of kinesin-mediated mitochondrial motility. *Cell* 136: 163–174.
59. Dubinsky JM, Levi Y (1998) Calcium-induced activation of the mitochondrial permeability transition in hippocampal neurons. *Journal of neuroscience research* 53: 728–741.
60. Hartmann H, Eckert A, Muller WE (1993) beta-Amyloid protein amplifies calcium signalling in central neurons from the adult mouse. *Biochemical and biophysical research communications* 194: 1216–1220.
61. Sberna G, Saez-Valero J, Beyreuther K, Masters CL, Small DH (1997) The amyloid beta-protein of Alzheimer's disease increases acetylcholinesterase expression by increasing intracellular calcium in embryonal carcinoma P19 cells. *Journal of neurochemistry* 69: 1177–1184.
62. Lin F, Wang Y, Hosford DA (1999) Age-related relationship between mRNA expression of GABA(B) receptors and calcium channel beta4 subunits in cacn4lh mice. *Brain research Molecular brain research* 71: 131–135.

63. Canevari L, Abramov AY, Duchen MR (2004) Toxicity of amyloid beta peptide: tales of calcium, mitochondria, and oxidative stress. *Neurochemical research* 29: 637–650.
64. Malaiyandi LM, Honick AS, Rintoul GL, Wang QJ, Reynolds IJ (2005) Zn<sup>2+</sup> inhibits mitochondrial movement in neurons by phosphatidylinositol 3-kinase activation. *The Journal of neuroscience : the official journal of the Society for Neuroscience* 25: 9507–9514.
65. Mattson MP (1994) Calcium and neuronal injury in Alzheimer's disease. Contributions of beta-amyloid precursor protein mistreatment, free radicals, and metabolic compromise. *Annals of the New York Academy of Sciences* 747: 50–76.
66. Mattson MP (1995) Free radicals and disruption of neuronal ion homeostasis in AD: a role for amyloid beta-peptide? *Neurobiology of aging* 16: 679–682; discussion 683.
67. Bus AI, Huang X, Fairlie DP (1999) The possible origin of free radicals from amyloid beta peptides in Alzheimer's disease. *Neurobiology of aging* 20: 335–337; discussion 339–342.
68. Kulisz A, Chen N, Chandel NS, Shao Z, Schumacker PT (2002) Mitochondrial ROS initiate phosphorylation of p38 MAP kinase during hypoxia in cardiomyocytes. *American journal of physiology Lung cellular and molecular physiology* 282: L1324–1329.
69. Semenova MM, Maki-Hokkonen AM, Cao J, Komarovski V, Forsberg KM, et al. (2007) Rho mediates calcium-dependent activation of p38alpha and subsequent excitotoxic cell death. *Nature neuroscience* 10: 436–443.
70. Arancio O, Zhang HP, Chen X, Lin C, Trinchese F, et al. (2004) RAGE potentiates Abeta-induced perturbation of neuronal function in transgenic mice. *The EMBO journal* 23: 4096–4105.
71. Chen KC, Kao PH, Lin SR, Chang LS (2008) p38 MAPK activation and mitochondrial depolarization mediate the cytotoxicity of Taiwan cobra phospholipase A2 on human neuroblastoma SK-N-SH cells. *Toxicology letters* 180: 53–58.
72. Kim S, Kim HY, Lee S, Kim SW, Sohn S, et al. (2007) Hepatitis B virus x protein induces perinuclear mitochondrial clustering in microtubule- and Dynein-dependent manners. *Journal of virology* 81: 1714–1726.
73. Thornton TM, Pedraza-Alva G, Deng B, Wood CD, Aronshtam A, et al. (2008) Phosphorylation by p38 MAPK as an alternative pathway for GSK3beta inactivation. *Science* 320: 667–670.
74. Li Z, Okamoto K, Hayashi Y, Sheng M (2004) The importance of dendritic mitochondria in the morphogenesis and plasticity of spines and synapses. *Cell* 119: 873–887.
75. Zenisek D, Matthews G (2000) The role of mitochondria in presynaptic calcium handling at a ribbon synapse. *Neuron* 25: 229–237.
76. Hollenbeck PJ (1996) The pattern and mechanism of mitochondrial transport in axons. *Frontiers in bioscience : a journal and virtual library* 1: d91–102.